Direct Observation of Domains in Model Stratum Corneum Lipid Mixtures by Raman Microspectroscopy

Aline Percot and Michel Lafleur
Département de Chimie and Groupe de Recherche en Transport Membranaire, Université de Montréal, Montréal, Québec H3C 3J7, Canada

ABSTRACT Several studies on intact and model stratum corneum (SC), the top layer of the epidermis, have suggested the presence of crystalline domains. In the present work, we used micro-Raman mapping to detect lipid domains in model lipid mixtures formed by an equimolar mixture of ceramides, cholesterol, and palmitic acid, the three main lipid species of SC. We were able to determine the spatial distribution of the three compounds individually based on the systematic analysis of band areas. As a control, we studied freeze-dried lipid mixtures, and the Raman microspectroscopy reported faithfully the homogeneous distribution of the three compounds. Spectral mapping was then performed on hydrated equimolar mixtures carefully annealed. In this case, clear phase separations were observed. Domains enriched in cholesterol, ceramides, or palmitic acid with a size of a few tens of square microns were detected. These findings constitute the first direct evidence of the formation of heterogeneous domains in the SC lipid models in a bulk phase. Raman microspectroscopy is an innovative approach to characterize the conditions leading to the formation of domains and provides new insights into the understanding of the skin barrier.

INTRODUCTION

The skin barrier has a fundamental role in the control of the exchanges with the external world. It has been established that the permeability properties are ensured by the stratum corneum (SC), the outermost layer of the epidermis (Elias, 1983). The SC is formed of corneocytes (mainly constituted of keratin), embedded within a lipid matrix. This macro-organization can be depicted as being somehow analogous to a brick wall where the corneocytes would be associated with the bricks and the lipids with the mortar (White et al., 1988). As the quality of the SC barrier is most likely dependent on the structure and composition of the intercellular lipid mortar (Onken and Moyer, 1963; Smith et al., 1982), their organization has been the subject of many investigations.

Over the last decades, several experimental techniques were exploited to investigate the morphology and the dynamics of this rather peculiar membrane to improve our understanding of the correlation between its structure and its functions. For example, small- and wide-angle x-ray diffraction (White et al., 1988; Parrott and Turner, 1993; Bouwstra et al., 1994, 1996; Bouwstra, 1997), differential scanning calorimetry (Wegener et al., 1996, 1997), spin label electron paramagnetic resonance (Alonso et al., 2000), NMR (Abraham and Downing, 1991; Fenske et al., 1994), Fourier transform infrared spectroscopy (Ongpipattanakul et al., 1994; Moore et al., 1997; Lafleur, 1998; Moore and Rerek, 2000), and Raman spectroscopy (Wegener et al., 1997; Lawson et al., 1998) have been used to elucidate the lipid organization in skin membranes. It is now established that the SC lipids form two lamellar phases with periodicity of the order of ~6 and 13 nm (White et al., 1988; Bouwstra et al., 1994; Bouwstra, 1997). The formation of crystalline domains within the lipid phase of the SC has been reported using x-ray diffraction (Bouwstra et al., 1994; Bouwstra, 1997) as well as infrared spectroscopy (Ongpipattanakul et al., 1994). Occasionally, diffraction peaks associated with crystalline cholesterol were observed (Parrott and Turner, 1993; Bouwstra et al., 1994).

As the SC lipids exhibit a complex and unusual lipid composition, biophysical studies are often performed on model mixtures to elucidate the role of each component in the mixture. These SC lipid model mixtures generally include the three main lipid species found in the SC lipid sheets, namely, ceramides, fatty acids, and cholesterol. Despite their simplicity, these model mixtures reproduce several features of the real SC lipid organization. For example, ordered-disordered phase transitions have been observed in these model mixtures at temperatures similar to those detected in SC lipids (Abraham and Downing, 1991; Kitson et al., 1994; Bouwstra et al., 1996; Moore et al., 1997; Lafleur, 1998). In addition, it has been shown by several techniques that at room temperature, these mixtures include a significant fraction of their lipids forming a solid or crystalline phase. Peaks corresponding to crystalline lipids were observed in the x-ray diffraction patterns of model mixtures (Parrott and Turner, 1993; Bouwstra et al., 1996). Deuterium-NMR spectroscopy has also shown the presence of solid cholesterol and fatty acid in mixtures including the three main lipid components of SC (Kitson et al., 1994; Fenske et al., 1994). Recent Fourier transform infrared spectroscopic studies of the ternary equimolar mixtures that included

Received for publication 21 December 2000 and in final form 19 June 2001.

Address reprint requests to Dr. Michel Lafleur, Département de Chimie, Université de Montréal, C.P. 6128, succursale Centre-ville, Montréal, Québec H3C 3J7, Canada. Tel.: 514-343-5936; Fax: 514-343-7586; E-mail: michel.lafleur@umontreal.ca.

0006-3495/01/10/2144/10 $2.00

perdeuterated palmitic acid showed evidence of phase-separated crystalline domains of ceramides and fatty acids with an orthorhombic chain packing (Moore et al., 1997; Lafleur, 1998; Moore and Rerek, 2000). This conclusion was inferred from the analysis of the methylene deformation and rocking bands, and it was also concluded from this approach that the domains would include at least 100 molecules and that their composition was at least 90% enriched in palmitic acid or ceramides. Finally, recent experiments in atomic force microscopy (AFM) on Langmuir-Blodgett monolayers formed with SC lipid model mixtures indicate phase separations leading to formation of domains that were proposed to be enriched in ceramides (ten Grotenhuis et al., 1996; Ekelund et al., 2000).

Forslind (1994) proposed that the organization of SC lipids can be described by crystalline domains surrounded with disordered grain border regions, forming "the domain mosaic model of the skin barrier." The presence of these micro-crystallites would be at the origin of the very small permeability of the skin. However, up to now, information about the organization, composition, and size of these proposed domains is still missing. A detailed characterization of the lipid organization would provide insights into the understanding of the skin permeability properties.

In the present paper, we examined by Raman microspectroscopy the lipid distribution of a widely studied model system made of an equimolar mixture of bovine brain ceramides, cholesterol, and palmitic acid, the three main compounds of SC. This mixture has revealed a rich polymorphism that shows similar features as those displayed by the intact SC (Kitson et al., 1994; Bouwstra et al., 1996). Raman spectroscopy is a precious tool to analyze lipid structure and organization (Wegener et al., 1996, 1997; Lawson et al., 1998; McCarthy et al., 2000) as the sampling requires no or little modification of the sample. The micro-Raman mapping allows the acquisition of chemical and morphological information over an area of the sample with a spatial resolution of the order of 1 μm. Using a visible laser light with an ordinary optical light microscope and a motorized X-Y stage, Raman spectra can be collected from small volume elements of a region of a sample and maps can be generated by analyzing characteristic bands. The analysis of the Raman spectra is rather complex as ceramides, cholesterol, and fatty acid give rise to similar vibrations appearing in the same spectral windows. To monitor individually palmitic acid, we used a perdeuterated fatty acid and to separate the ceramides and the cholesterol contributions in the C-H stretching vibration ($\nu_{C\text{-}H}$) region, we used curve fitting to obtain a calibration curve using characteristic bands. D_2O-based buffer was used with a pH of 5.3 corresponding to the physiological pH of the SC layer (Öhman and Vahlquist, 1994).

Using micro-Raman mapping, we investigated the phase behavior of a ternary equimolar mixture of ceramides, cholesterol, and palmitic acid, freeze-dried and hydrated. The freeze-dried mixture is used as a control for the method as it is supposed to be homogeneous, whereas phase separation is expected in the hydrated mixture.

MATERIALS AND METHODS

Bovine brain ceramides (type III) (Cer), cholesterol (Chol), and 2-*N*-morpholinoethanesulfonic acid (Mes) buffer were purchased from Sigma Chemical Co. (St. Louis, MO). Perdeuterated palmitic acid (PA-d_{31}) was obtained from CDN Isotopes (Pointe-Claire, Canada) and EDTA from Aldrich (Milwaukee, WI).

To obtain the lipid mixtures, a stock solution of each lipid was prepared in a benzene/methanol mixture, 95/5 (v/v) for cholesterol and palmitic acid and 90/10 (v/v) for ceramides. Appropriate volumes of the solutions were mixed to obtain the desired lipid composition, and the organic solutions were then freeze-dried. The resulting powder should have preserved the random distribution of the molecular species that existed in the organic solutions.

For the hydrated samples, the solid lipids were hydrated with a large excess ($\sim$30 mg ml^{-1}) of buffer (100 mM Mes buffer, containing 100 mM NaCl, 5 mM EDTA, in D_2O, at pH 5.3). A D_2O-based buffer was used because it provides a Raman signal (the O-D stretching mode located at 2200–2850 cm^{-1}) between the C-H (2750–3100 cm^{-1}) and the C-D stretching (1900–2250 cm^{-1}) bands. This band that is useful to examine the hydration of the samples limits the spectral window that had to be scanned. In addition, because the proper incubation of the samples was verified by the profile of the amide I′ band of the infrared (IR) spectra (Lafleur, 1998), the D_2O-based buffer prevented the strong spectral interference of water in the amide I region. The samples were incubated for three 10-min periods at 80°C. Between incubation periods, the samples were vortexed and cooled down to room temperature. The samples were finally incubated at 36°C for at least 1 h before Raman mapping. The proper annealing of the samples was verified as described previously (Lafleur, 1998) by recording the IR spectrum of an aliquot of the mixture and by verifying that the amide I′ region included the three components that were associated with the thermodynamically stable phase of the ternary mixture at low temperatures.

Raman spectroscopy

The Raman spectra were recorded using a Renishaw Raman Imaging Microscope WiRE (V1.2) (System 3000) (Renishaw, Gloucestershire, UK) containing a holographic grating (1800 grooves mm^{-1}), a Leica microscope equipped with a long-working-distance objective with magnification factor of $\times$50, and a Peltier cooled CCD detector (600 $\times$ 400 pixels). The spectra were excited by the 514.5-nm line of an argon ion (Ar^+) laser. The laser power at the sample was $\sim$1 mW. The diameter of the beam with the optical set-up used for the data collection was $\sim$2.5 μm, as measured on its reflection on a silicon surface. This configuration led to a spectral resolution of $\sim$2 cm^{-1}. The spectra were recorded at room temperature. These systems have been shown to remain in a very ordered phase up to 40°C (Kitson et al., 1994; Moore et al., 1997; Lafleur, 1998). Therefore, the recorded spectra are typical of this lipid state.

For anhydrous samples, the lipids were spread between a microscope glass slide and a glass cover. In the case of hydrated samples, the wax-like mixture was transferred with an excess of buffer in a homemade sealed Teflon cell that included a glass cover; this set-up was necessary to ensure maintaining the sample hydration.

For the mapping, spectra were recorded between 1900 and 3200 cm^{-1} in the continuous mode. The acquisition of each spectrum required $\sim$30 s, and the digital resolution was one data point/1.6 cm^{-1}. To investigate the spatial distribution of the three compounds, the sample was moved by a computer-controlled translational stage. Typically, a surface of 40 μm $\times$ 40 μm was scanned by moving the sample by 1-μm steps. Therefore, 1681

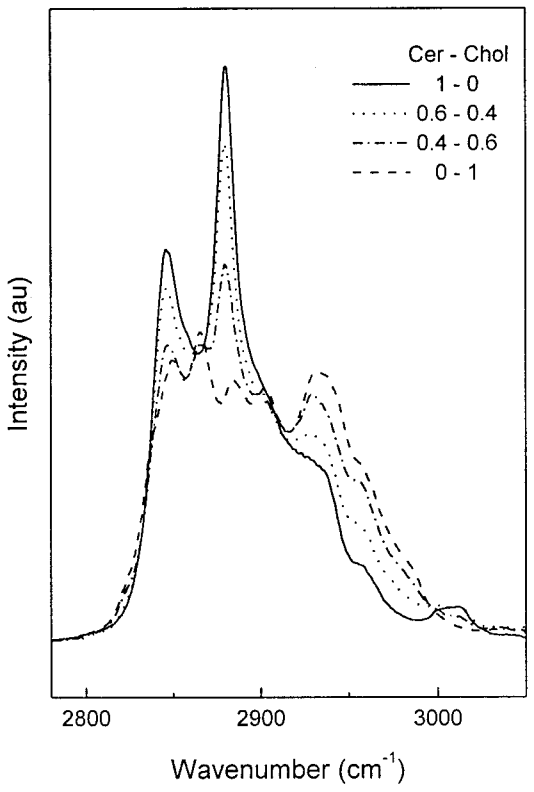

FIGURE 1 Raman spectra of various anhydrous Cer-Chol mixtures with defined molar ratio, normalized to the same total area.

spectra were recorded over the surface, for a total acquisition time of ~16 h. Maps were then generated by integrating the area of characteristic bands as described below. The data analysis and the map generation were performed using GRAMS/32 (Galactic Industries Corp., Salem, NH) and the WiRE software (version 1.3) (Renishaw Spectroscopy Products Division).

RESULTS AND DISCUSSION

Before the analysis of the Raman mapping of the SC models, the Raman spectra of each compound were recorded. Ceramides and cholesterol both absorb in the same spectral windows. For example, the $\nu_{C\text{-}H}$ region of the Raman spectra of pure ceramides and cholesterol as well as of some dry binary mixtures of these chemicals are displayed in Fig. 1. For both ceramides and cholesterol, the bands around 2845 and 2880 cm^{-1} are associated with the symmetric and antisymmetric CH_2 vibration stretching modes (ν_sCH_2 and ν_aCH_2) (Bulkin and Krishnan, 1971; Faiman, 1977; Williams et al., 1992; McCarthy et al., 2000). The bands at 2895 and 2930 cm^{-1} of the ceramides spectra have been associated with a broad contribution due to Fermi resonance involving the chain terminal CH_3 symmetric stretching (v_sCH_3) mode and binary combinations or overtones of the CH_2 deformations modes (Williams et al., 1992; McCarthy et al., 2000). The band at 2865 cm^{-1} in the cholesterol spectrum has been associated to the ν_sCH_3 mode whereas the band at 2902 cm^{-1} was assigned to methyl on the steroid rings or ternary C-H (Bulkin and Krishnan, 1971). The contribution at 2930 cm^{-1} probably arises from a contribution of both CH_2 and CH_3 groups in the cholesterol molecules. The other bands of the spectra could not be attributed unambiguously from the literature.

TABLE 1 Curve-fitting parameters for the 2794–2980-cm^{-1} region

Peak number	Center (cm^{-1})	Width (cm^{-1})	% Lorentzian
1	2842–2852	≥14	0–0.5
2	2855–2872	≥14	0–0.5
3	2875–2890	≥14	0–0.5
4	2890–2906	31.5	0
5	2928–2938	31.5	0
6	2950–3050	31.5	0

The Raman spectra of Cer-Chol mixtures are complex owing to the overlap of the Raman bands in the spectra of the two compounds. The mixture spectra can actually be simulated by a linear combination of the individual spectra in the appropriate proportions. The additive property of the spectra implies that, in these solid mixtures, there is no significant changes in the spectra that would be associated with intermolecular interactions because the C-H (as well as the C-D) stretching modes are sensitive to the acyl chain conformational order (Mantsch and McElhaney, 1991; Wegener et al., 1997; Lawson et al., 1998; McCarthy et al., 2000). Because of the spectral additivity, the proportion of cholesterol in a sample can be estimated from the subtraction of the cholesterol spectrum from the spectrum of the mixture to obtain a spectrum similar to that of pure ceramides, once the spectral intensities have been normalized. However, we have found that this approach is rather subjective and difficult to implement on a spectral cube that can contain over 1600 spectra. On Fig. 1, one can observe that the relative areas of several bands in the $\nu_{C\text{-}H}$ region are modified as a function of the cholesterol content in the mixtures. The $\nu_{C\text{-}H}$ region includes at least six components that can be identified from the visual inspection of the spectra. Therefore, we have attempted to simulate this region (2794–2980 cm^{-1}) of all these spectra with a mathematical curve-fitting procedure, using six bands described as mixtures of Gaussian and Lorentzian functions. To obtain reproducible results and to limit the occurrence of mathematical solutions that are unreasonable from a spectroscopic point of view, some parameters were fixed or allowed to vary within a limited range. The limitations imposed on the parameters are displayed in Table 1. The spectral window associated with the position of each component was selected to ensure that one and only one band would be found where components are seen in the spectra. The width and the percentage of Lorentzian of the peaks 1, 2, and 3 were allowed to vary in a limited range. The shape of the com-

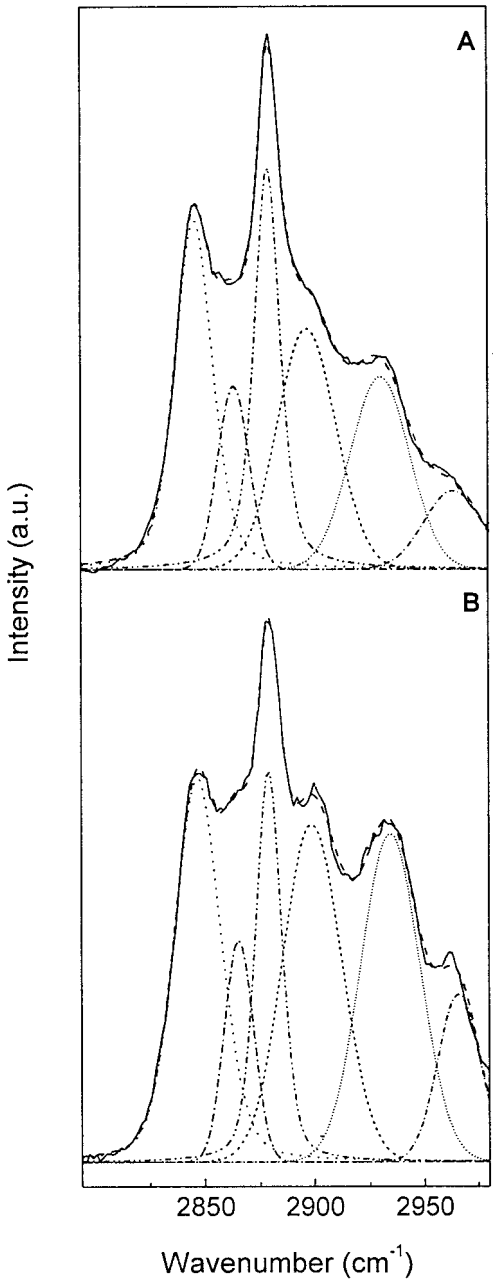

FIGURE 2 Experimental (—) and simulated (— — —) Raman spectra for hydrated Cer-Chol-PA-d_{31} mixtures in the $\nu_{C\text{-}H}$ region with *A* and *B* corresponding to a ceramide- and a cholesterol-rich domain, respectively.

ponents 4, 5, and 6 was Gaussian and their width was fixed to 31.5 cm^{-1} as small changes in peaks 4 and 6 influence considerably the area of peak 5 (at ~2930 cm^{-1}), the peak selected to probe the cholesterol content. These limitations have always provided reasonable solutions for all the treated spectra (over 10,000 spectra). The band-fitting results obtained for two samples with different cholesterol content are shown in Fig. 2.

It was found that the area of peak 5 located around 2930 cm^{-1} (A_{2930}) could be used as a probe for the cholesterol

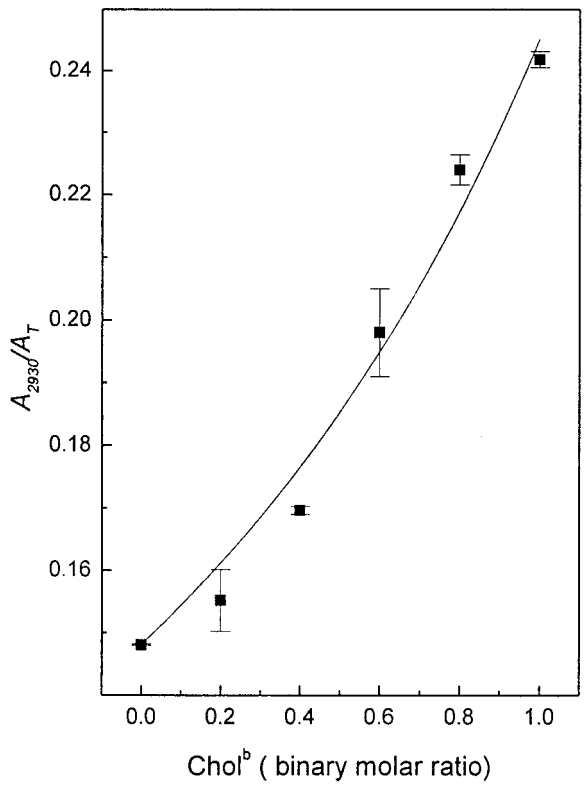

FIGURE 3 Calibration curve to determine the cholesterol content. A_{2930}/A_T represents the area ratio of the simulated band around 2930 cm^{-1} over the total $\nu_{C\text{-}H}$ region area in the Raman spectra of anhydrous binary Cer-Chol mixtures. The variation of A_{2930}/A_T as a function of cholesterol molar ratio ($Chol^b$) is represented. The error bars represent the standard deviation on the results obtained from at least three spectra recorded on different spots of the samples. The solid line represents the fit obtained according to Eq. 1A.

content. This area was expressed relative to the total area of the $\nu_{C\text{-}H}$ region (A_T), integrated between 2780 and 3100 cm^{-1}. The quantitative correlation existing between the contribution of the cholesterol in the $\nu_{C\text{-}H}$ region as expressed by the A_{2930}/A_T ratio and the proportion of cholesterol in the binary Cer-Chol model mixtures, expressed by $Chol^b$ (the superscript b refers to the binary mixture) is plotted in Fig. 3. The results indicate that the contribution of the band at 2930 cm^{-1} increases progressively with the cholesterol molar fraction. It should be noted that this molar fraction is expressed relative to the quantity of ceramides and cholesterol and does not take into account the deuterated fatty acid. The relationship was described by a rational function and could be fitted with the following equation:

$$\frac{A_{2930}}{A_T} = \frac{0.1481 + 0.004 \times Chol^b}{1 - 0.38 \times Chol^b} \qquad (1A)$$

This equation relating the A_{2930}/A_T ratio and the proportion of cholesterol can be reorganized to provide a relationship

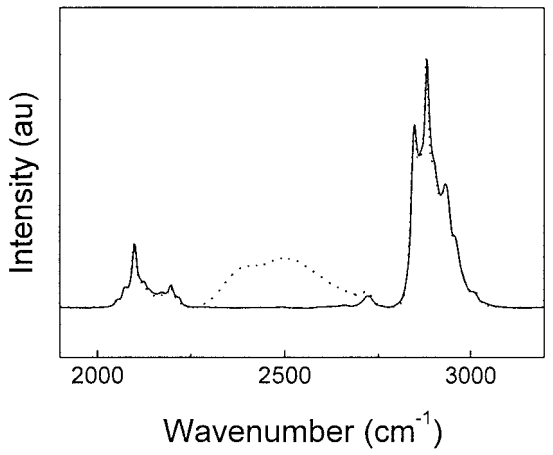

FIGURE 4 The 1900–3200-cm^{-1} regions of the mean Raman spectra for freeze-dried (—) and hydrated (— — —) Cer-Chol-PA-d_{31} equimolar mixtures, averaged over the map.

allowing us to evaluate the proportion of cholesterol from the A_{2930}/A_T ratio obtained from a spectrum:

$$\text{Chol}^b = \frac{\frac{A_{2930}}{A_T} - 0.1481}{0.004 + 0.38 \times \frac{A_{2930}}{A_T}} \quad (1B)$$

This approach was applied to our spectral cubes to estimate the cholesterol and ceramides molar fractions over the surface analyzed by Raman mapping.

We have examined the lipid distribution in the freeze-dried and the hydrated equimolar mixture of Cer-Chol-PA-d_{31}. For each sample, a spectral cube composed of 1681 Raman spectra collected over a 1600-μm^2 surface (i.e., about one spectrum per 1 μm^2). The spectra resulting from the averaging over all the spectra recorded for one sample of the dry and the hydrated mixtures are displayed in Fig. 4. As expected, both spectra are very similar as the mixtures have the same composition. The symmetric and antisymmetric CD_2 stretching modes ($\nu_s CD_2$ and $\nu_a CD_2$) arising from the deuterated fatty acid are observed at 2100 and 2175 cm^{-1}, respectively. This region also includes the symmetric CD_3 stretching mode ($\nu_s CD_3$), which gives rise to two components at 2120 and 2075 cm^{-1}, this splitting being attributed to an interaction with the overtone of the asymmetric CD_3 deformation mode at 1058 cm^{-1} (Mendelsohn et al., 1976; Bryant et al., 1982). The C-H stretching region between 2750 and 3100 cm^{-1} shows a similar profile to those recorded for equimolar mixtures of ceramides and cholesterol. The spectra obtained for the dry and the hydrated samples are very similar, the main difference being the appearance of the O-D stretching band associated with D_2O at around 2500 cm^{-1}. As the methylene and methyl stretching regions are sensitive to chain order (Mantsch and McElhaney, 1991; Wegener et al., 1997; Lawson et al., 1998; McCarthy et al., 2000), the similarity of the band profiles in the C-H and C-D stretching regions indicates that the hydration does not lead to considerable changes of acyl chain order. This result is in agreement with previous results obtained by IR (Moore et al., 1997; Lafleur, 1998) and ^2H NMR (Abraham and Downing, 1991; Fenske et al., 1994) spectroscopy, indicating highly ordered acyl chains in the hydrated samples.

To investigate the spatial distribution of each component in the sample, a systematic and objective analysis of the Raman spectra has been applied. First, maps were obtained by integration of the areas of three characteristic regions: 1) the 2780–3100-cm^{-1} region, which is associated with the $\nu_{C\text{-}H}$ of both cholesterol and ceramides (Map($\nu_{C\text{-}H}$)); 2) the area of peak 5 at 2930 cm^{-1} as obtained from the curve-fitting procedure in the $\nu_{C\text{-}H}$ region (Map(A_{2930})), which was used to quantify the cholesterol content; and 3) the 2015–2250-cm^{-1} region, which is associated with the $\nu_{C\text{-}D}$ of PA-d_{31} (Map($\nu_{C\text{-}D}$)) (maps not shown).

To determine the molar fractions of each component from the spectrum associated with each sampling element, the molar fraction relative only to cholesterol and ceramides, Chol^b and Cer^b, were first calculated from the $\nu_{C\text{-}H}$ region. A map was obtained by dividing the area of peak 5 (Map(A_{2930})) over the total area of the $\nu_{C\text{-}H}$ band (Map($\nu_{C\text{-}H}$)) for each element. These ratios are proportional to Chol^b in the system based on the Eq. 1A; the values of Chol^b and Cer^b ($1 - \text{Chol}^b$) of each sampling element were calculated using this relationship leading to the Map(Chol^b) and Map(Cer^b).

To determine the PA-d_{31} content, Raman intensity ratios were used as the C-H stretching modes are mainly associated with ceramides and cholesterol, whereas the C-D stretching region is associated with the palmitic acid. The absolute Raman intensity could vary significantly between the sampling elements because some parameters, such as the quantity of material and the optical properties associated with each element, were not identical. This variation in the C-H region was taken into account by performing the following normalization procedure. First, the maps Map(Chol^b) and Map(Cer^b) were multiplied by Map($\nu_{C\text{-}H}$). Two maps were thus obtained, Map(A_{Chol}) and Map(A_{Cer}), corresponding to relative areas representative of the molar fractions of cholesterol and ceramides, respectively, and of the absolute Raman intensity measured for each element. The average values over Map(A_{Chol}) and Map(A_{Cer}) were practically equal because cholesterol and ceramide were equimolar in the mixture. Second, to determine the PA-d_{31} content, the absolute intensities of the $\nu_{C\text{-}D}$ region had to be normalized as the C-D stretching modes are less active than the equivalent C-H stretching modes. The areas associated with the $\nu_{C\text{-}D}$ region (Map($\nu_{C\text{-}D}$)) were first multiplied by a constant to obtain the same average area value over this map as the average area values over Map(A_{Chol}) and Map(A_{Cer}). This operation was associated with the fact that each com-

ponent was in equimolar proportion and, therefore, an equivalent Raman intensity over the whole investigated surface was assigned. The generated map was referred to as Map($\nu_{C\text{-}D}^{corr}$) This normalization factor had to be slightly adjusted for each sampling element because the ($\nu_{C\text{-}D}$ band area/$\nu_{C\text{-}H}$ band area) ratio is slightly dependent on the molar fraction of ceramide and cholesterol contributing in the C-H stretching region. To determine this correction of the area normalization, we recorded the spectra of ternary mixtures containing different molar fractions of cholesterol ($Chol^b$) and ceramide (Cer^b), but always 50(mol)% of PA-d_{31} to provide an internal intensity standard. The graph of the total area of the $\nu_{C\text{-}H}$ band, normalized relative to that measured when $Chol^b$ was 0.5, as a function of $Chol^b$ was linear (data not shown), and the linear least-squares fit was

$$\frac{\text{Area of the } \nu_{C-H} \text{ band}}{\text{Area of the } \nu_{C-H} \text{ band for } (Chol^b = 0.5)} = -0.466\ Chol^b + 1.233. \quad (2A)$$

To provide a more accurate normalization of the C-D region, the areas associated with the Map($\nu_{C\text{-}D}^{corr}$) were multiplied by the factor taking into account the variations of $Chol^b$. Over the maps, this correction was on the order of 10%. A map corresponding to palmitic acid (Map(A_{PA})) was therefore obtained from

$$\text{Map}(A_{PA}) = \text{Map}(\nu_{C-D}^{corr}) \times [-0.466\ \text{Map}\ (Chol^b) + 1.233]. \quad (2B)$$

The molar fractions of cholesterol, ceramides, and palmitic acid in the ternary mixture ($Chol^t$, Cer^t, PA^t) for each sampling element could therefore be calculated using the following equations:

$$\text{Map}(Cer^t) = \frac{\text{Map}(A_{Cer})}{\text{Map}(A_{Cer}) + \text{Map}(A_{Chol}) + \text{Map}(A_{PA})}$$

$$\text{Map}(Chol^t) = \frac{\text{Map}(A_{Chol})}{\text{Map}(A_{Cer}) + \text{Map}(A_{Chol}) + \text{Map}(A_{PA})}$$

$$\text{Map}(PA^t) = \frac{\text{Map}(A_{PA})}{\text{Map}(A_{Cer}) + \text{Map}(A_{Chol}) + \text{Map}(A_{PA})} \quad (3)$$

Three maps corresponding to the molar fractions of cholesterol (Map($Chol^t$)), ceramides (Map(Cer^t)), and palmitic acid (Map(PA^t)) in the ternary mixture were obtained for the freeze-dried and the hydrated samples (Fig. 5). The average value obtained over these three maps for the freeze-dried, and the hydrated sample is ~0.33. The gray scale was established to cover ±25% of the average value obtained over the whole map. For the freeze-dried sample, the distribution of the three components was rather homogeneous as shown by the homogeneously gray map. On the other hand, the hydrated and incubated sample showed a much more contrasted signal. For each of the three components, the maps showed some regions enriched (lighter) or depleted (darker) in one type of lipid. The lipid distributions obtained for the two types of samples are shown on Fig. 6. In the case of the freeze-dried homogeneous mixture (Fig. 6, *A–C*), we observe a narrow distribution centered near 0.33. The lipid composition distributions were fitted with a Gaussian curve, and the mean value obtained was 0.33 with a standard deviation of 0.02. This result indicates that the freeze-dried mixture displays a homogeneous lipid distribu-

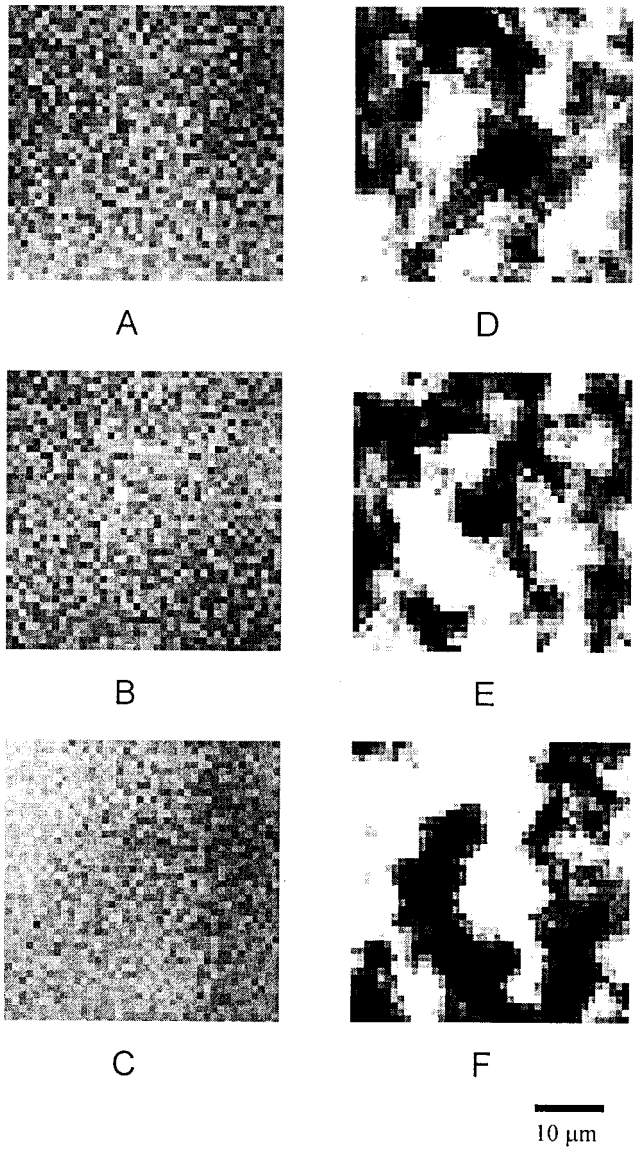

FIGURE 5 Raman maps corresponding to cholesterol (*A* and *D*), ceramides (*B* and *E*) and palmitic acid (*C* and *F*) molar fraction maps ((Map($Chol^t$), Map(Cer^t) and Map(PA^t)) for the Cer-Chol-PA-d_{31} equimolar mixtures collected over an area of 40 × 40 μm^2. Freeze-dried (*A–C*) and hydrated (*D–F*) mixtures. The gray scale covers 25% on either sides of the average value over the whole map.

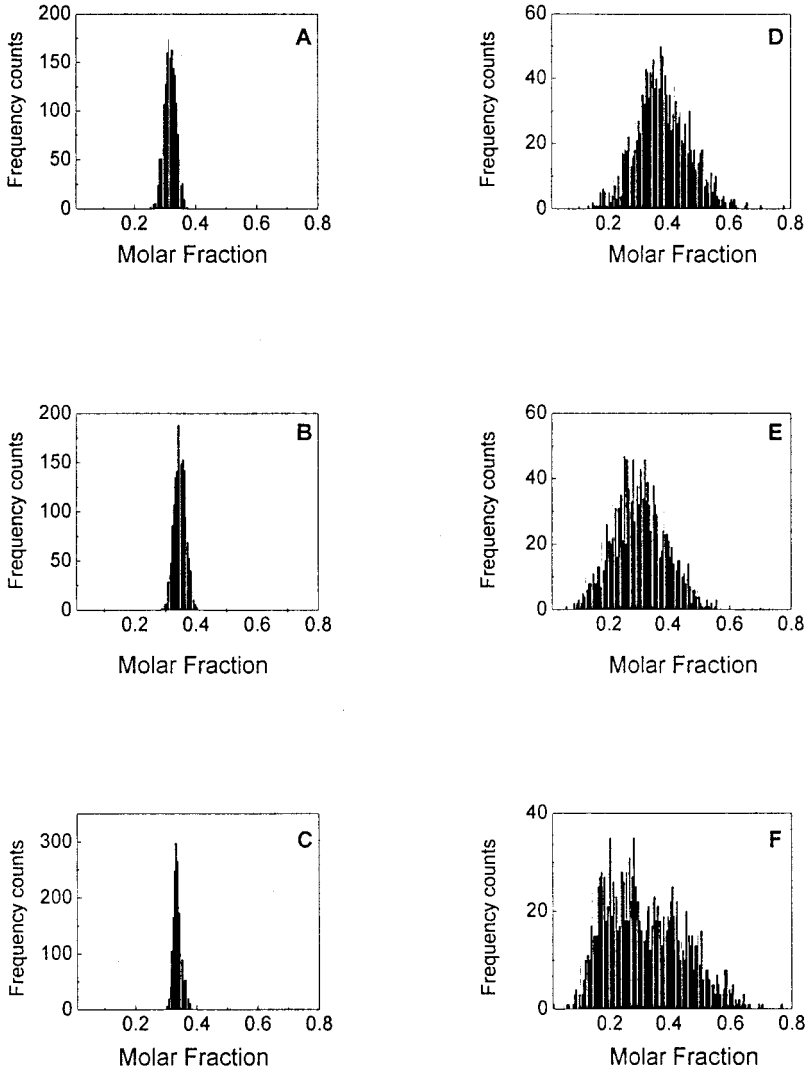

FIGURE 6 Histograms representing the distribution of the molar fractions of the freeze-dried (*A–C*) and hydrated (*D–F*) Cer-Chol-PA-d_{31} equimolar mixtures determined over the investigated area ($40 \times 40\ \mu m^2$). *A* and *D*, *B* and *E*, and *C* and *F* correspond, respectively, to the molar fraction of cholesterol, ceramides, and palmitic acid.

tion and also validates our spectral data-processing procedure. In the case of cholesterol and ceramides, the distribution is slightly larger than in the case of palmitic acid, which can be explained by the fact that the separation of the respective cholesterol and ceramides contribution is not as straightforward as that of palmitic acid. Fig. 6, *D—F*, shows the distribution of the molar fraction values for the hydrated mixture. The average molar fraction is indeed $\sim 0.32 \pm 0.04$ for each component, but the composition distribution of the hydrated sample is much larger than for the anhydrous mixture. Conversely to the freeze-dried mixtures for which the palmitic acid distribution was the narrowest, it is the widest for the hydrated samples. This component is the easiest to locate because of the isotopic shift, and therefore the related results are likely more accurate. About 75% of the sampling elements in the hydrated samples correspond to domains whose composition is different by 25% or more from the average value obtained over the whole map, i.e., elements that can be considered as enriched or depleted in one component.

The phase separation phenomenon in the hydrated SC lipid model mixtures can be highlighted by overlapping the maps representing the enriched domains in one particular lipid. In this case, a volume element defined as enriched in one given lipid species was marked with a given color. The operational definition of enriched element that we used was a sampling element with a molar fraction in one species greater by 25% or more than the average value, i.e., a molar fraction higher than ~ 0.41 in one species. In the freeze-dried sample, no such element could be observed as illustrated by the molar fraction distributions (Figs. 5 and 6, *A–C*). As the lipids are freeze-dried together from an organic solution, the resulting powder is homogeneous. The results obtained with the hydrated samples are shown in Fig. 7 *A*. The map is the result of the superimposition of the three maps Map($Chol^t$), Map(Cer^t), and Map(PA^t) represented on Fig. 5, *D–F*, where domains were colored according to their major component and regions without any dominant component were left black. Several domains enriched in cholesterol, ceramides, or palmitic acid are observed. The do-

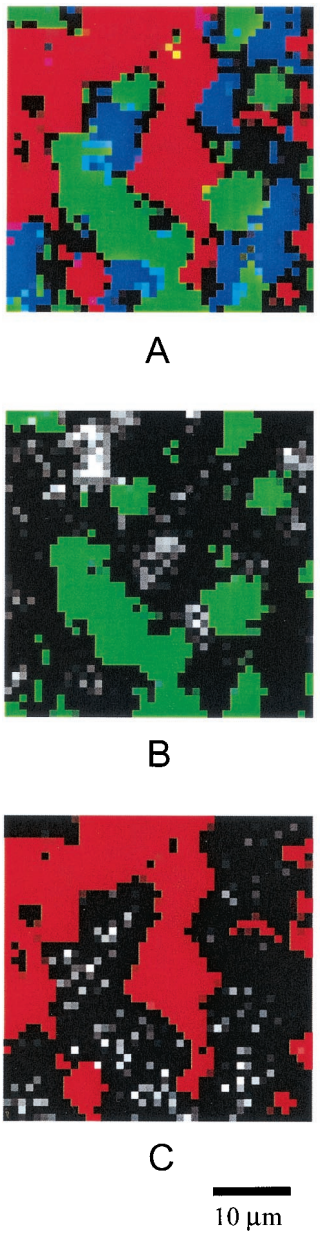

FIGURE 7 (*A*) Superimposition of the cholesterol-rich (blue), ceramide-rich (green), and palmitic-acid-rich (red) domains. (*B* and *C*) Superposition of the 2880-cm^{-1} band width values and the ceramide-rich domains (*B*) and of the 2100-cm^{-1} band width values with the palmitic-acid-rich domains (*C*). The width, measured at half height, of the 2880- and 2100-cm^{-1} bands are displayed using a gray scale from 14 to 16 cm^{-1} and 17 to 20 cm^{-1}, respectively. In the spectral fitting, the standard error associated with the band width was ~0.4 cm^{-1}.

mains do not appear to have a well defined shape. The enriched domains for each single component cover ~24 ± 8% of the surface scanned (21% for ceramides, 17% for cholesterol, and 33% for palmitic acid). If a domain were defined as a series of sampling elements with at least one adjacent side, the average size and the standard deviation would be 26 ± 48 μm^2 for ceramides, 23 ± 26 μm^2 for

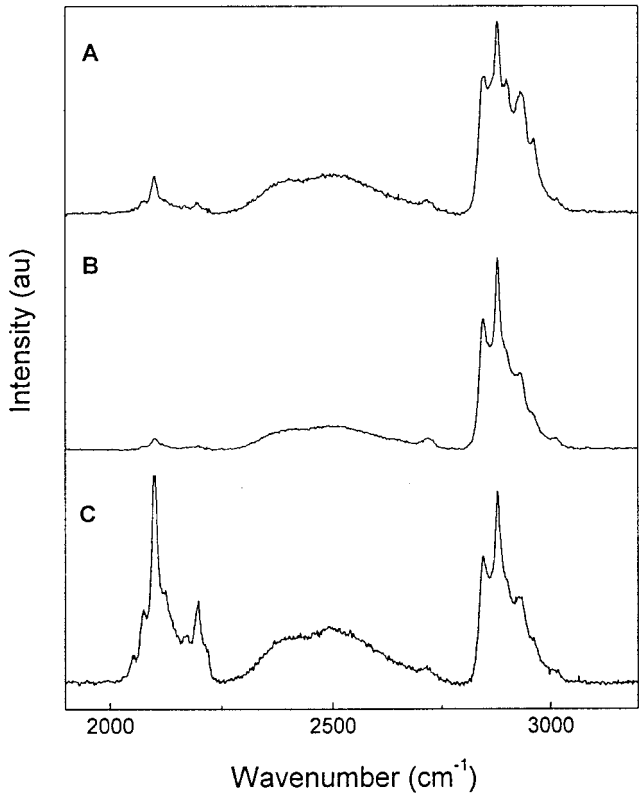

FIGURE 8 Raman spectra of a hydrated Cer-Chol-PA-d_{31} equimolar mixture in the 1900–3200-cm^{-1} region in cholesterol-rich (*A*), ceramide-rich (*B*), and palmitic-acid-rich (*C*) domains.

cholesterol, and 56 ± 149 μm^2 for palmitic acid. Spectra extracted from cholesterol-, ceramides-, and palmitic-acid-rich regions are displayed on Fig. 8, *A–C*. These examples of raw data clearly support the conclusions reached from the systematic spectral analysis. The visual inspection of the spectra convincingly shows the enrichment in a specific component.

As it is well established that the CH_2 and CD_2 stretching modes can be used to measure the degree of order of the alkyl chain, the disorder of the C-H and C-D chains was estimated by measuring the band widths at 2880 and 2100 cm^{-1} (Mendelsohn and Koch, 1980; Kouaouci et al., 1985; Wegener et al., 1996, 1997; Lawson et al., 1998; McCarthy et al., 2000). The bandwidths were obtained by curve-fitting procedures. In the case of C-H stretching, the width-at-half-height ($\Delta\nu_{1/2}$CH) of the peak 3 (Table 1) was used to estimate the ceramides order. For the analysis of the C-D stretching region, a curve-fitting procedure was performed using the parameters described in Table 2. The $\Delta\nu_{1/2}$CD of peak 3, located around 2100 cm^{-1}, was used to probe the palmitic acid order. An increase in these bandwidths is generally associated with less ordered acyl chains. Two maps were obtained with each pixel representing the width of a methylene stretching band (Fig. 7, *B* and *C*). The changes in width were limited. However, in some areas,

TABLE 2 Curve-fitting parameters for the 2014–2204-cm^{-1} region

Peak number	Center (cm^{-1})	Width (cm^{-1})	% Lorentzian
1	2045–2055	1–40	0–0.5
2	2068–2078	1–40	0–0.5
3	2093–2103	1–40	0–0.5
4	2116–2126	1–40	0–0.5
5	2138–2148	1–40	0–0.5
6	2168–2178	1–40	0–0.5
7	2191–2201	1–40	0–0.5

components with significantly greater width could be observed. In Fig. 7 *B*, the map representing the hydrogenated acyl chain disorder inferred from the 2880-cm^{-1} band was superimposed to the map showing the ceramides-rich domains, and in Fig. 7 *C*, the map representing the deuterated acyl chain disorder, inferred from the 2100-cm^{-1} band, was superimposed to the map showing the deuterated palmitic-acid-rich domains. The more disordered lipids were generally found outside the enriched domains, in the neighboring regions. These maps support the existence of crystalline domains surrounded by a more fluid lipid matrix.

The proposition of domains with heterogeneous lipid composition is consistent with recent results obtained on similar mixtures. IR studies (Moore et al., 1997; Lafleur, 1998; Moore and Rerek, 2000) have reported the formation of crystalline domains enriched in palmitic acid or ceramides. Because the splitting measured for the methylene deformation and rocking bands had the maximum values, it was proposed that the domains would be formed of almost pure palmitic acid or ceramides. In our maps, no volume element showed a molar fraction in one component higher than 0.80. However, it should be noted that IR spectroscopy and Raman microspectroscopy operate in different spatial regimes. The IR vibrational splitting indicates that domains of at least 100 chains are formed but is insensitive to larger scale. In Raman microspectroscopy, the sampling element is at the microscopic scale, i.e., much larger than 100 lipid chains. Despite the resolution on the order of 2 μm in the plan perpendicular to the laser beam, the thickness of the sampled area was $\sim$20 μm (data not shown). Therefore, the values displayed in the maps are averages over these microscopic volume elements, and it is likely that they include relatively pure domains and mixed peripheral lipids, which would lead to averaged enrichment factors. The observation of domains in the micro-Raman maps is conclusively associated with the phase separation reported by IR spectroscopy and provides details relative to their size, morphology, and arrangement. Using AFM, some regions with a height greater by $\sim$8 Å than the rest of a monolayer formed with a Cer-Chol-PA mixture were observed (ten Grotenhuis et al., 1996). These domains were interpreted as almost pure ceramide, more specifically those with long chains that are found in the bovine brain ceramides used in that study like in the present investigation. The composition of the rest of the monolayer was therefore inferred to be composed of cholesterol, palmitic acid, and only the short-chain ceramides. The size and the shape of the ceramide domains observed in that study are comparable to the ceramide-enriched domains that we have identified. Because the height of cholesterol and palmitic acid molecules is relatively similar, it is not clear whether AFM would distinguish domains enriched in one of the two components. Another AFM study showed the formation of small rectangular domains in monolayers prepared from cholesterol and ceramides (Ekelund et al., 2000). These domains were interpreted as ceramides domains surrounded by a cholesterol-rich phase. Even though the sample preparation and composition were considerably different compared with our experiments, phase separations in monolayers and in bulk phase appear to be an emerging feature of the SC lipids.

CONCLUSIONS

In the present work, micro-Raman mapping was successfully used to probe the phase separation in Cer-Chol-PA-d_{31} equimolar mixtures. We observed directly the presence of domains enriched in each component of the ternary mixture. The presented findings support the domain mosaic model that has been proposed as the architectural basis of the skin barrier (Forslind, 1994). The presented picture here is actually reminiscent of a structure where the enriched domains are mainly crystalline and the surrounding mixed regions would form fluid edges. As the effective barrier property of the SC has been related to the ordered arrangement of the intercellular lipids (Golden et al., 1987; Potts and Francoeur, 1990), a better understanding of the role of each lipid in governing the barrier function of mammalian skin would greatly improve our comprehension of skin disease and transdermal drug delivery (Knutson et al., 1985). It is necessary to identify the role played by various molecular parameters such as acyl chain mismatch and hydrogen-bonding capabilities at the headgroup level. The possibility of visualizing the domain formation by obtaining a spatial and chemical description of lipid mixtures by micro-Raman spectroscopy constitutes a powerful approach to gain insights into these issues.

We thank Marjolaine Arseneault for her valuable help during the revision of the manuscript. The financial support from the Natural Sciences and Engineering Research Council (NSERC) of Canada and Fonds FCAR from the Province of Quebec is gratefully acknowledged.

REFERENCES

Abraham, W., and D. T. Downing. 1991. Deuterium NMR investigation of polymorphism in stratum corneum lipids. *Biochim. Biophys. Acta.* 1068: 189–194.

Alonso, A., N. C. Meirelles, and M. Tabak. 2000. Lipid chain dynamics in stratum corneum studied by spin label electron paramagnetic resonance. *Chem. Phys. Lipids.* 104:101–111.

Bouwstra, J. A. 1997. The skin barrier, a well-organized membrane. *Colloids Surf. A.* 123–124:403–413.

Bouwstra, J. A., G. S. Gooris, K. Cheng, A. Weerheim, W. Bras, and M. Ponec. 1996. Phase behavior of isolated skin lipids. *J. Lipid Res.* 37:999–1011.

Bouwstra, J. A., G. S. Gooris, J. A. van der Spek, S. Lavrijsen, and W. Bras. 1994. The lipid and protein structure of mouse stratum corneum: a wide and small angle diffraction study. *Biochim. Biophys. Acta.* 1212:183–192.

Bryant, G. J., F. Lavialle, and I. W. J. Levin. 1982. Effects of membrane bilayer reorganizations on the 2103 cm^{-1} Raman spectral C-D stretching mode linewidths in dimyristoyl phosphatidylcholine-d_{54} (DMPC-d_{54}) liposomes. *J. Raman Spectrosc.* 12:118–121.

Bulkin, B. J., and K. Krishnan. 1971. Vibrational spectra of liquid crystals. III. Raman spectra of crystal, cholesteric, and isotropic cholesterol esters, 2800–3100-cm^{-1} region. *J. Am. Chem. Soc.* 17:5998–6004.

Ekelund, K., L. Eriksson, and E. Sparr. 2000. Rectangular solid domains in ceramide-cholesterol monolayers: 2D crystals. *Biochim. Biophys. Acta.* 1464:1–6.

Elias, P. M. 1983. Epidermal lipids, barrier function, and desquamation. *J. Invest. Dermatol.* 80:44s–49s.

Faiman, R. 1977. Raman spectroscopic studies of different forms of cholesterol and its derivatives in the crystalline state. *Chem. Phys. Lipids.* 18:84–104.

Fenske, D. B., J. L. Thewalt, M. Bloom, and N. Kitson. 1994. Model of stratum corneum intercellular membranes: ^2H NMR of macroscopically oriented multilayers. *Biophys. J.* 67:1562–1573.

Forslind, B. 1994. A domain mosaic model of the skin barrier. *Acta Dermatol. Venereol.* 74:1–6.

Golden, G. M., D. B. Guzek, A. H. Kennedy, J. E. McKie, and R. O. Potts. 1987. Stratum corneum lipid phase transitions and water barrier properties. *Biochemistry.* 26:2382–2388.

Kitson, N., J. Thewalt, M. Lafleur, and M. Bloom. 1994. A model approach to the epidermal permeability barrier. *Biochemistry.* 33:6707–6715.

Knutson, K., R. O. Potts, D. B. Guzek, G. M. Golden, J. E. McKie, W. J. Lambert, and W. I. Higuchi. 1986. Macro- and molecular physical-chemical considerations in understanding drug transport in the stratum corneum. *J. Controlled Release.* 2:67–87.

Kouaouci, R., J. R. Silvius, I. Graham, and M. Pézolet. 1985. Calcium-induced lateral phase separations in phosphatidylcholine-phosphatidic acid mixtures. A Raman spectroscopic study. *Biochemistry.* 24: 7132–7140.

Lafleur, M. 1998. Phase behaviour of model stratum corneum lipid mixtures: an infrared spectroscopy investigation. *Can. J. Chem.* 76: 1501–1511.

Lawson, E. E., A. N. C. Anigbogu, A. C. Williams, B. W. Barry, and H. G. M. Edwards. 1998. Thermally induced molecular disorder in human stratum corneum lipids compared with a model phospholipid system: FT-Raman spectroscopy. *Spectrochim. Acta A.* 54:543–558.

Mantsch, H. H., and R. N. McElhaney. 1991. Phospholipid phase transitions in model and biological membranes as studied by infrared spectroscopy. *Chem. Phys. Lipids.* 57:213–226.

McCarthy, P. K., C.-H. Huang, and I. W. Levin. 2000. Raman spectroscopic study of polycrystalline mono- and polyunsaturated 1-eicosanoyl-d_{39}-2-eicosenoyl-*sn*-glycero-3-phosphocholines: bilayer lipid clustering and acyl chain order and disorder characteristics. *Biopolymers.* 57:2–10.

Mendelsohn, R., and C. C. Koch. 1980. Deuterated phospholipids as Raman spectroscopic probes of membrane structure: phase diagrams for the dipalmitoyl phosphatidylcholine(and its d_{62} derivative)-dipalmitoyl phosphatidylethanolamine system. *Biochim. Biophys. Acta.* 598: 260–271.

Mendelsohn, R., S. Sunder, and H. J. Bernstein. 1976. Deuterated fatty acids as Raman spectroscopic probes of membrane structure. *Biochim. Biophys. Acta.* 443:613–617.

Moore, D. J., and M. E. Rerek. 2000. Insights into the molecular organization of lipids in the skin barrier from infrared spectroscopy studies of stratum corneum lipid models. *Acta Dermatol. Venereol. Suppl.* 208: 16–22.

Moore, D. J., M. E. Rerek, and R. Mendelsohn. 1997. Lipid domains and orthorhombic phases in model stratum corneum: evidence from Fourier transform infrared spectroscopy studies. *Biochem. Biophys. Res. Commun.* 231:797–801.

Öhman, H., and A. Vahlquist. 1994. In vivo studies concerning a pH gradient in human stratum corneum and upper epidermis. *Acta Dermatol. Venereol.* 74:375–379.

Ongpipattanakul, B., M. L. Francoeur, and R. O. Potts. 1994. Polymorphism in stratum corneum lipids. *Biochim. Biophys. Acta.* 1190: 115–122.

Onken, H. D., and C. A. Moyer. 1963. The water barrier in human epidermis. *Arch. Dermatol.* 87:584–590.

Parrott, D. T., and J. E. Turner. 1993. Mesophase formation by ceramides and cholesterol: a model for stratum corneum lipid packing? *Biochim. Biophys. Acta.* 1147:273–276.

Potts, R. O., and M. L. Francoeur. 1990. Lipid biophysics of water loss through the skin. *Proc. Natl. Acad. Sci. U.S.A.* 87:3871–3873.

Smith, W. P., M. S. Christensen, S. Nacht, and E. H. Gans. 1982. Effect of lipids on the aggregation and permeability of human stratum corneum. *J. Invest. Dermatol.* 78:7–11.

ten Grotenhuis, E., R. A. Demel, M. Ponec, D. R. Boer, J. C. van Miltenburg, and J. A. Bouwstra. 1996. Phase behavior of stratum corneum lipids in mixed Langmuir-Blodgett monolayers. *Biophys. J.* 71: 1389–1399.

Wegener, M., R. Neubert, W. Rettig, and S. Wartewig. 1996. Structure of stratum corneum lipids characterized by FT-Raman spectroscopy and DSC. I. Ceramides. *Int. J. Pharmacol.* 128:203–213.

Wegener, M., R. Neubert, W. Rettig, and S. Wartewig. 1997. Structure of stratum corneum lipids characterized by FT-Raman spectroscopy and DSC. III. Mixtures of ceramides and cholesterol. *Chem. Phys. Lipids.* 88:73–82.

White, S. H., D. Mirejovsky, and G. I. King. 1988. Structure of lamellar lipid domains and corneocyte envelopes of murine stratum corneum: an x-ray diffraction study. *J. Am. Chem. Soc.* 27:3725–3732.

Williams, A. C., H. G. M. Edwards, and Barry, B. W. 1992. Fourier transform Raman spectroscopy: a novel application for examining human stratum corneum. *Int. J. Pharmacol.* 81:R11–R12.